



**HAL**  
open science

## Potential-Induced Fine-Tuning of the Enantioaffinity of Chiral Metal Phases

Sunpet Assavapanumat, Thittaya Yutthalekha, Patrick Garrigue, Bertrand Goudeau, Veronique Lapeyre, Adeline Perro, Neso Sojic, Chularat Wattanakit, Alexander Kuhn

► **To cite this version:**

Sunpet Assavapanumat, Thittaya Yutthalekha, Patrick Garrigue, Bertrand Goudeau, Veronique Lapeyre, et al.. Potential-Induced Fine-Tuning of the Enantioaffinity of Chiral Metal Phases. *Angewandte Chemie International Edition*, 2019, 58 (11), pp.3471-3475. 10.1002/anie.201812057 . hal-02509463

**HAL Id: hal-02509463**

**<https://hal.science/hal-02509463v1>**

Submitted on 16 Mar 2020

**HAL** is a multi-disciplinary open access archive for the deposit and dissemination of scientific research documents, whether they are published or not. The documents may come from teaching and research institutions in France or abroad, or from public or private research centers.

L'archive ouverte pluridisciplinaire **HAL**, est destinée au dépôt et à la diffusion de documents scientifiques de niveau recherche, publiés ou non, émanant des établissements d'enseignement et de recherche français ou étrangers, des laboratoires publics ou privés.

## Potential Induced Fine-tuning the Enantioaffinity of Chiral Metal Phases

Sunpet Assavapanumat, Thittaya Yutthalekha, Patrick Garrigue, Bertrand Goudeau, Véronique Lapeyre, Adeline Perro, Neso Sojic, Chularat Wattanakit,\* and Alexander Kuhn\*

**Abstract:** Concepts leading to single enantiomers of chiral molecules are of crucial importance for many applications, including pharmacology and biotechnology. Recently, mesoporous metal phases encoded with chiral information have been developed. We propose here to fine-tune the enantioaffinity of such structures by imposing an electric potential, which can influence the electrostatic interactions between the chiral metal and the target enantiomer. This allows increasing the binding affinity and thus the discrimination between two enantiomers. The concept is illustrated by generating chiral encoded metals in a microfluidic channel via the reduction of a platinum salt in the presence of a liquid crystal and L-tryptophan as a chiral model template. After removal of the template molecules, the modified microchannel retains a pronounced chiral character. Its chiral recognition efficiency can be fine-tuned by applying a suitable potential to the metal phase. This enables the separation of both components of a racemate flowing through the channel. The approach constitutes a promising and complementary strategy in the frame of chiral discrimination technologies.

Chiral molecules are ubiquitous in nature and also of tremendous importance in artificial (supra)molecular systems. Although they exhibit the same physical and chemical properties, very different biological activities are often observed for two enantiomers. One enantiomer might have beneficial effects when used as a drug, whereas the other one acts as a toxic compound. Therefore, the scientific community has made enormous efforts to obtain enantiomerically pure compounds and in this context the development of synthesis and separation technologies to produce single enantiomers is a key challenge for pharmaceutical applications.[1] Various strategies have been employed to minimize the effect of unwanted enantiomeric compounds, e.g. chiral analysis,[2] asymmetric synthesis[3] and chiral separation.[4] The latter can be achieved using different technologies, including rather classic chiral selectors on stationary phases, or more exotic but very exciting recent approaches based on magnetic field effects, with the potential advantage of being very versatile.[4i] However, the majority of these concepts relies on materials bearing chiral features. Such materials can be obtained, among others, by molecular imprinting,[2e, 5], molecular grafting[6], molecular adsorption[7] or by using organometallic[3b] and metal organic framework[8] compounds. Molecular imprinting is a very popular approach, which employs an enantiomer as an asymmetric template to create a material with chiral cavities.[9] Although molecularly imprinted polymers (MIPs) have been widely used in chiral recognition experiments by mimicking biologically active sites,[10] they may have some drawbacks, such as a difficult removal of the template or a restricted access of the target molecule to the imprinted cavity.[11]

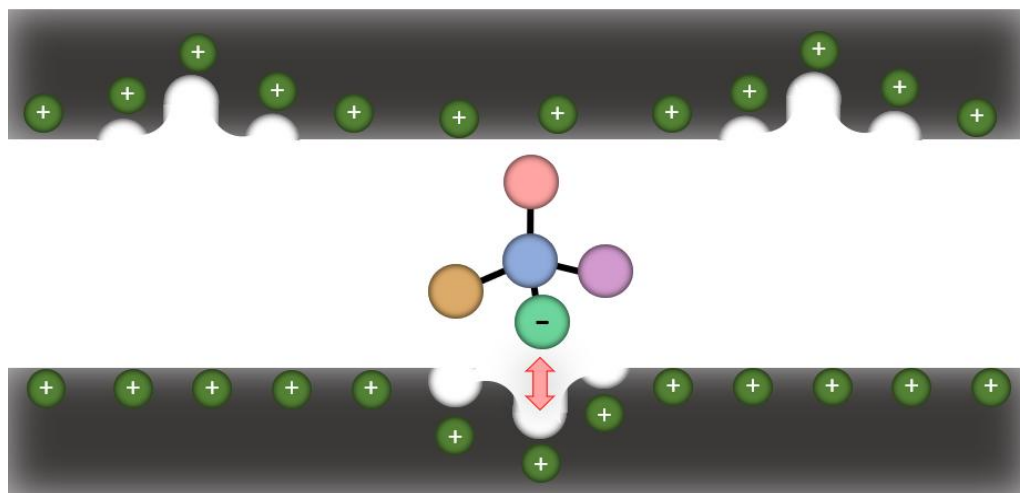
These disadvantages can be partially circumvented when introducing an additional porosity in the material.[12] Following an analogous philosophy, chiral-imprinted platinum films have been recently developed using electrodeposition in the presence of a self-assembled lyotropic liquid crystalline phase as a template to create a mesoporous structure.[13] In the case of the simultaneous presence of a target enantiomer, molecular cavities with chiral features can be generated in the mesopores.[14] The developed materials have been used for applications ranging from chiral recognition and electroanalysis[14a] to asymmetric synthesis.[14b,14d] Such chiral imprinted

mesoporous metal surfaces (CIMMS) combine in a synergetic way a very high active surface area and promising enantioselective recognition and synthesis abilities.

The binding affinity of a molecule for a given surface can be significantly improved by controlling the involved interactions, such as hydrogen bonding or electrostatic forces. With respect to the latter one, capillary electrochromatography is a good example to illustrate the separation of molecules in the presence of an electric field.[15,16,17] The applied potential allows enhancing electrostatic interactions with the surface of the stationary phase, eventually exalting the discrimination of two enantiomers.[4c, 16]

In order to combine the attractive features of CIMMS with the benefits of controlling electrostatic interactions between chiral molecules and solid surfaces, we propose here to fine-tune the affinity of chiral molecules for mesoporous chiral platinum deposited in a microfluidic channel by adjusting its electrochemical potential. In this case the CIMMS is acting simultaneously as a working electrode and as a stationary phase. The potential needs to be optimized, because too low potentials might not generate a sufficient electrostatic force, whereas too high potentials may lead to a degradation of the target molecule, the solvent or the metal structure.[14c]

This concept of controllable enantioaffinity is exemplified in the present contribution by using L-tryptophan (L-Trp) as a model compound, because it is a well-known essential amino acid, involved in protein synthesis, and a precursor of the neurotransmitter serotonin, whereas its mirror image, D-tryptophan (D-Trp), is used in pharmaceutical applications as an intermediate in the synthesis of peptide antibiotics.



Scheme 1. Schematic illustration of the electrostatic interaction of deprotonated tryptophan with a cavity in a positively charged mesopore of the microchannel.

Under the present experimental conditions (pH=10-11) tryptophan is deprotonated and therefore negatively charged. Its interaction with the imprinted cavity of a positively polarized metal surface is illustrated in Scheme 1. The electrostatic interaction is expressed by the Coulombic force (FE), related to the potential E applied to the CIMMS and the charge q of the target molecule.

$$F_E = qE \quad (1)$$

This force enhances the interaction between tryptophan and the chiral metal structure, thus facilitating the discrimination between the two components of a racemic mixture. The chiral platinum film in the microchannel is prepared following an adapted literature procedure (Figure S1

and Supplementary Information).[14c] In brief, a self-assembled lyotropic liquid crystal phase, which is interacting with the chiral template molecule and the metal salt, is deposited on a gold-coated glass slide. After the electroreduction of the metal salt in the presence of the template by injecting a given amount of charge, the electrode is washed to liberate the mesopores and the imprinted chiral cavities. The resulting deposit of tryptophan-imprinted mesoporous platinum can then be characterized by scanning electron microscopy (SEM) and shows a very homogeneous surface (Figures 1a and 1b).

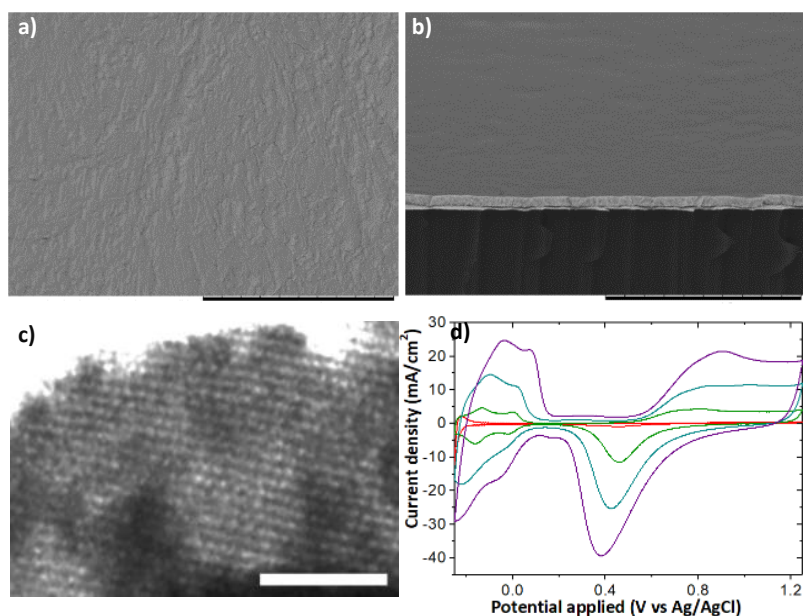
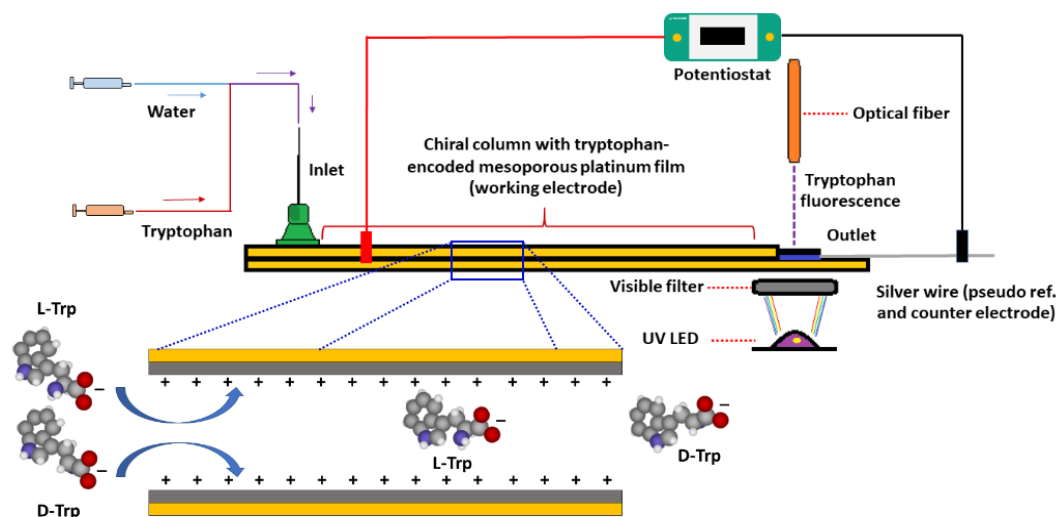


Figure 1. (a) and (b) Scanning electron microscopy images of L-Trp encoded mesoporous platinum deposited with  $8 \text{ C cm}^{-2}$  as top view and cross section, respectively. Scale bar 100 and  $20 \mu\text{m}$ . (c) Transmission electron microscopy image of the platinum film. Scale bar  $50 \text{ nm}$ . (d) Cyclic voltammograms of various platinum electrodes in  $0.5 \text{ M H}_2\text{SO}_4$  at  $100 \text{ mVs}^{-1}$  in the range of  $-0.25$  to  $1.25 \text{ V vs Ag/AgCl}$ : (red) flat platinum; (green), (blue) and (purple) Trp-encoded mesoporous platinum deposited with 2, 4 and  $8 \text{ C cm}^{-2}$ .

The mesoporous structure was confirmed by transmission electron microscopy, revealing a typical pore size of around  $2 \text{ nm}$  (Figure 1c). The electroactive surface of the platinum films obtained for various deposition charge densities was measured in  $0.5 \text{ M}$  sulfuric acid in the range of  $-0.25$  to  $1.25 \text{ V vs Ag/AgCl}$ , based on the area of the peaks associated with hydrogen adsorption and desorption (Figure 1d). This is the standard procedure to evaluate electrochemically the real surface area. It becomes obvious that the active surface of the mesoporous platinum electrodes is almost two orders of magnitude higher compared to flat platinum. The calculated surface enhancement correlates in a linear way with the injected charge density ( $16$ ,  $35$  and  $82$  for  $2$ ,  $4$  and  $8 \text{ C.cm}^{-2}$ , respectively, Figure S2).

To confirm the enantioselective recognition properties, the oxidation of L-Trp and D-Trp at the porous platinum electrodes was tested: using differential pulse voltammetry (DPV) in the Trp oxidation region from  $0.7$  to  $1.2 \text{ V vs Ag/AgCl}$  (Figure S3). The chiral character of the metal phase can be deduced from the amplitude of current density in the Trp oxidation region. As expected, no chiral recognition is found in the case of non-encoded flat platinum, because both enantiomers are able to interact in an identical way with the flat surface (Figure S3a). In strong contrast to this, the platinum electrode imprinted with L-Trp preferentially converts L-Trp on its surface rather than the D-Trp

species, as demonstrated by the higher oxidation signal (Figure S3b). On the other hand, for the D-Trp imprinted platinum electrode, the amplitude of current density in a D-Trp solution is significantly higher than the one in a L-Trp solution (Figure S3c). In order to exclude that experimental artefacts lead to these observations, the chiral information can be electrochemically erased by scanning the potential of both electrodes to rather high positive values in sulfuric acid. In this case platinum is oxidized and the chiral imprints are lost. Testing the electrodes afterwards again in their respective Trp solutions results in equal oxidation currents (Figure S3d). In addition, platinum imprinted by Trp enantiomers also exhibits significant recognition properties in the case of the oxidation of 3,4-dihydroxy-phenylalanine (DOPA) enantiomers (Figure S4). This is comparable to what has been already observed for electrodes imprinted with mandelic acid.[14a]



**Scheme 2.** Hyphenated microfluidic electrochromatography device with a L-Trp-encoded mesoporous platinum film as stationary phase. The electrochemical potential of the stationary phase is controlled by a potentiostat.

In order to illustrate the benefits of the chiral imprinted metal films for the separation of enantiomers, the designed materials were electrochemically deposited as the equivalent of a stationary phase in a micro-fluidic channel. This allows injecting a small volume of a racemic mixture at the entrance of the channel and then flushing it over the CIMMS by pumping continuously the aqueous mobile phase. At the outlet (Scheme 2 and Figure S5) the released molecules are detected by fluorescence measurements at 396 nm, performed with an optical fiber connected to a spectrophotometer, and a UV-LED excitation at 260 nm (Absorption and emission spectra of tryptophan are shown in Figure S6). The big advantage of a metallic stationary phase is that it can be simultaneously used as an electrode and its potential can be controlled with respect to an external reference electrode during the residence time of the chiral molecules in the channel. This allows a fine-tuning of the electrostatic interactions between the enantiomers and the imprinted chiral cavities. When using the L-tryptophan imprinted mesoporous platinum as a stationary phase and as an electrode, the applied potential can be controlled by a potentiostat connected to the supporting gold plate and to an external silver wire, the latter being positioned at the channel outlet, acting as a counter and pseudo reference electrode.

The applied potential was optimized in order to find the most suitable condition in terms of separation efficiency (Figure 2). Trp injection was first carried out without applied potential as a blank experiment with a flow rate of 0.5 ml min<sup>-1</sup> (Figure 2a). This leads to a broad peak compared to the injection of a single enantiomer, because the interactions are not pronounced enough to allow baseline separation. In contrast, when a potential of +200 mV vs Ag is applied to the mesoporous metal layer, the electrostatic interactions between the negatively charged amino acid and the

positively charged channel walls are enhanced. As illustrated in Figure 2b, this globally prolongs the residence time of the mixture as the mean retention time without potential is around 600s, whereas with applied potential it moves to a global value of 800s. However, both enantiomers are not affected equally. The stronger interaction of L-Trp with the imprinted chiral cavities results in a very significant prolongation of its retention time (peak at 1200s), whereas D-Trp is almost unaffected within the error bars of the measurement. This can be explained as follows.

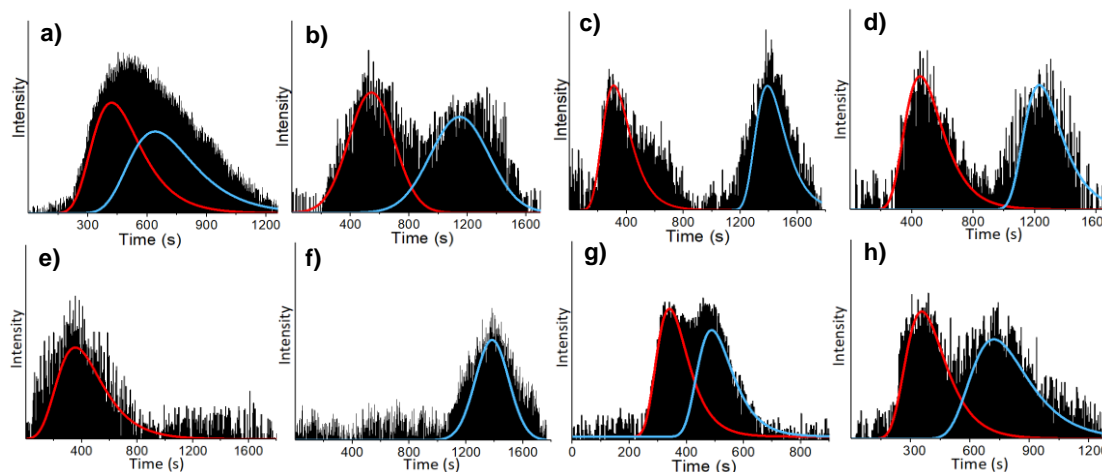


**Figure 2.** Electrochromatograms of racemic Trp solutions with fluorescence detection at the microchannel outlet by an optical fiber for a L-Trp imprinted platinum layer. (a) No applied potential; (b) +200 mV vs Ag; (c) and (d) +300 mV vs Ag with a freshly prepared layer and after 1 month, respectively; (e) and (f) +300 mV vs Ag and injection of the single enantiomers D-Trp and L-Trp, respectively. Separation of Naproxen enantiomers on a L-Trp-encoded platinum film at g) +300 mV and h) +400 mV vs Ag.

When a chiral imprinted metal is exposed to a racemic mixture there exists a partition coefficient between the outer solution and the inner metal phase, which is significantly in favor of the imprinted enantiomer, as we could show already in a previous study.[14c] This means that the majority of the chiral cavities inside the mesoporous structure are occupied with one type of enantiomer, namely the imprinted one. When a positive electric potential is applied to the metal phase these molecules in the cavities will be retained much longer, whereas the opposite enantiomer, which is preferentially present in the solution phase outside of the metal (see the channel configuration in Figure S5b) will not be affected, thus explaining the almost unchanged retention time. This allows a partial separation of the two molecules at the outlet. When the potential is increased to +300 mV, the racemate is totally separated as shown in Figure 2c, with a peak maximum again around ~400 s for D-Trp (Figure 2e), followed by L-Trp at ~1400 s (Figure 2f). In summary, L-Trp has already an attractive interaction with the imprinted sites even in the absence of electric field (see the broad peak in Figure 2a), and this binding becomes stronger when the positive potential increases. In contrast, D-Trp is initially not recognized by the cavities and therefore, even when applying a positive potential, the retention is more or less identical.

Applying too positive potentials might increase the risk to trigger real electrochemical reactions in the column, such as oxidizing the platinum surface, inducing a rearrangement of platinum atoms and thus a loss of enantioselectivity. However, as we show, using only moderate positive potentials is already sufficient for base-line separation and prevents degrading the chiral features of the microchannel, illustrated by Figure 2d, which has been recorded after one month with the same microchannel as in Figure 2c.

Previously we could demonstrate that imprinting platinum with a given chiral compound confers the metal layer also a certain enantioselectivity with respect to other chiral compounds during electroanalysis.<sup>14a</sup> We have tested this feature also in the present case of chiral separation. In order to demonstrate the versatility of the approach, the L-Trp imprinted layer was also used for separating another enantiomer. Due to the detection by fluorescence in the present set-up, the choice of amino acids is limited, because they need to provide a significant fluorescence signal. This is the case for Tyrosine (Tyr). Almost no separation of Tyr racemate is observed when no potential is applied. Only a slight shoulder indicates the presence of two enantiomers (Figure S7a). However, when the electrostatic interaction is tuned by applying a potential of +300 mV, a significant difference in retention time is obtained for the two enantiomers (Figure S7b). Even without further optimization this leads to almost baseline separation, indicating that although the metal has been imprinted with Trp, it is able to differentiate the two Tyr stereoisomers.

A similar behaviour is recorded when studying the pharmaceutical compound Naproxen with the same chiral metal phase. Without applying a potential no separation is observed (Figure S8), whereas Figures 2g and 2h demonstrate that even for this compound, which is quite different in terms of molecular structure when compared to the imprinted Trp, a significant enantioaffinity appears when an increasingly positive potential is applied. It is therefore possible to imagine a broader spectrum of chiral molecules which can be separated by one and the same metal phase.

In summary, fine-tuning the potential of these chiral metal phases allows for the first time a successful separation of enantiomers. No separation is observed when racemic Trp is injected into a microchannel coated with a L-Trp encoded porous platinum film without applying potential. A gradual increase of potential leads to baseline separation. This study describes a straight-forward concept allowing the design of new stationary phases for electrochromatography where the enantioaffinity can be adjusted on-demand. For the moment, the non-optimized life-time of such deposits is exceeding one month and therefore opens up very interesting perspectives in the field of chiral separation.

#### Experimental Section

For experimental details, please see the Supporting informations.

#### Acknowledgements

We would like to thank Simon Hemour, Jean-Luc Lachaud and Olivier Nguyen for advice and technical assistance and Sopon Butcha and the Vidyasirimedhi Institute of Science and Technology (VISTEC) FRC for TEM characterization. This work was supported by the bilateral PICS program of CNRS. A.K. is grateful to the Institut Universitaire de France for financial support. Chu. W. thanks the Thailand Research Fund (TRF) (MRG6180099). S.A. acknowledges a Ph.D. cotutelle scholarship from Campus France, the French Embassy in Thailand and VISTEC. This project has also been funded by the European Research Council (ERC) under the European Union's Horizon 2020 research and innovation program (grant agreement n° 741251, ERC Advanced grant ELECTRA).

Keywords: enantioselectivity • chiral discrimination • molecular imprinting • mesoporous metal • electrochromatography

[1] a) D. Cheng, Y. Ishihara, B. Tan, C. F. Barbas. *ACS Catal.* 2014, 4, 743-762. b) S. Fanali. *J. Chromatogr. A.* 2000, 875, 89-122. c) E. R. Francotte. *J. Chromatogr. A.* 2001, 906, 379-397.

[2] a) I. Mogi, K. Watababe. *Chem. Lett.* 2012, 41, 1439-1441. b) H. Caner, E. Groner, L. Levy. *Drug. Discov. Today.* 2004, 9, 105-110. c) K. Haupt. *Analyst.* 2001, 126, 747-756. d) S. Arnaboldi, M.

Magni, P. R. Mussini. *Curr. Opin. Electrochem.* 2018, 8, 60-72. e) M. C. Blanco-López, M. J. Lobo-Castañón, A. J. Miranda-Ordieres, P. Tuñón-Blanco. *Biosens. Bioelectron.* 2003, 18, 353-362. f) B. Petrie, R. Barden, B. Kasprzyk-Hordern. *Water. Res.* 2015, 72, 3-27. g) N. Berova, L. Di Bari, G. Pescitelli. *Chem. Soc. Rev.* 2007, 36, 914-931.

[3] a) O. Ramstrom, R. J. Ansell. *Chirality.* 1998, 195-209. b) D. Sinou. *Adv. Synth. Catal.* 2002, 344, 221-237. c) R. Giri, B. F. Shi, K. M. Engle, N. Maugel, J. Q. Yu. *Chem. Soc. Rev.* 2009, 38, 3242-3272. d) T. Akiyama, J. Itoh, K. Fuchibe. *Adv. Synth. Catal.* 2006, 348, 999-1000. e) D. Chen, Y. Wang, J. Klankermayer. *Angew. Chem.* 2010. 122, 9665-9668. f) E. J. Corey, C. J. Helal. *Angew. Chem. Int. Ed.* 1998. 37, 1986-2012.

[4] a) G. Gubitz, M. G. Schmid. *J. Chromatogr. A.* 2008, 1204, 140-156. b) T. J. Ward, K. D. Ward. *Anal. Chem.* 2010, 82, 4712-4722. c) L. Schweitz, L. I. Andersson, S. Nilsson. *Anal. Chem.* 1997, 69, 1179-1183. d) T. Takeuchi, J. Haginaka. *J. Chromatogr. B.* 1999, 728, 1-20. e) M. Kempe, K. Mosbach, J. Chromatogr. A. 1995, 691, 317-323. f) N. B. Maier, P. Franco, W. Lindner. *J. Chromatogr. A.* 2001, 906, 3-33. g) B. R. Hart, D. J. Rush, K. J. Shea. *J. Am. Chem. Soc.* 2000, 122, 460-465. h) V. Schurig, D.P. Nowotny. *Angew. Chem. Int. Ed. Engl.* 1990. 29, 939-957. i) K. B. Ghosh, O. B. Dor, F. Tassinari, E. Capua, S. Yocheles, A. Capua, S. H. Yang, S. S. P. Parkin, S. Sarkar, L. Kronik, L. T. Baczewski, B. Naaman, Y. Paltiel. *Science*, 2018, 360, 1331-1334.

[5] a) C. Alexander, H. S. Andersson, L. I. Andersson, R. J. Ansell, N. Kirsch, I. A. Nicholls, J. O'Mahony, M. J. Whitcombe. *J. Mol. Recognit.* 2006, 19, 106-180. b) C. Wattanakit, *Curr. Opin. Electrochem.* 2018, 7, 54-60. c) L. Duran Pachon, I. Yosef, T. Z. Markus, R. Naaman, D. Avnir, G. Rothenberg. *Nat. Chem.* 2009, 1, 160-164. d) R. B. Pernites, S. K. Venkata, B. D. Tiu, A. C. Yago, R. C. Advincula. *Small.* 2012, 8, 1669-1674. e) G. Attard, M. Casadesus, L. E. Macaskie, K. Deplanche, *Langmuir.* 2012, 28, 5267-5274. f) M. J. Whitcombe, M. E. Rodriguez, P. Villar, E. N. Vulfson. *J. Am. Chem. Soc.* 1995, 117, 7105-7111. g) Z. Zhang, X. Zhang, B. Liu, J. Liu, *J. Am. Chem. Soc.* 2017, 139, 5412-5419.

[6] a) S. Edmondson, V. L. Osborne, W. T. Huck. *Chem. Soc. Rev.* 2004, 33, 14-22. b) P. C. Mondal, C. Fontanesi, R. Naaman. *ACS Nano.* 2015, 9, 3377-3384.

[7] a) I. Lee, F. Zaera. *J. Phys. Chem.* 2005, 109, 12920-12926. b) I. Lee, F. Zaera, *J. Am. Chem. Soc.* 2006, 128, 8890-8898.

[8] M. Padmanaban, P. Muller, C. Lieder, K. Gedrich, R. Grunker, V. Bon, I. Senkovska, S. Baumgartner, S. Opelt, S. Paasch, E. Brunner, F. Glorius, E. Klemm, S. Kaskel. *Chem. Commun.* 2011, 47, 12089-12091.

[9] a) K. Mosbach. *Tech.* 1994, 19, 9-14. b) M. Kempe, K. Mosbach. *J. Chromatogr. A.* 1995, 694, 3-13.

[10] a) E. Turiel, A. Martin-Esteban. *Anal. Chim. Acta.* 2010, 668, 87-99. b) F. Puoci, F. Iemma, N. Picci. *Curr. Drug. Deliv.* 2008, 5, 85-96.

[11] L. Chen, S. Xu, J. Li. *Chem. Soc. Rev.* 2011, 40, 2922-2942.

[12] a) M. Dabrowski, M. Cieplak, K. Noworyta, M. Heim, W. Adamkiewicz, A. Kuhn, P. S. Sharma, W. Kutner. *J. Mat. Chem. B.* 2017, 5, 6292-6299. b) M. Dabrowski, M. Cieplak, P. S. Sharma, P. Borowicz, K. Noworyta, W. Lisowski, F. D'Souza, A. Kuhn, W. Kutner, *Biosens. Bioelectron.* 2017, 94, 155-161.



- [13] G. S. Attard, P. N. Bartlett, N. R. B. Coleman, J. M. Elliott, J. R. Owen, J. H. Wang. *Science*. 1997, 28, 838-840.
- [14] T. Yutthalekha, C. Warakulwit, J. Limtrakul, A. Kuhn, *Electroanal.* 2015, 27, 2209-2213. b) T. Yutthalekha, C. Wattanakit, V. Lapeyre, S. Nokbin, C. Warakulwit, J. Limtrakul, A. Kuhn. *Nat. Commun.* 2016, 7, 12678. c) C. Wattanakit, Y. B. Come, V. Lapeyre, P. A. Bopp, M. Heim, S. Yadnum, S. Nokbin, C. Warakulwit, J. Limtrakul, A. Kuhn. *Nat. Commun.* 2014, 5, 3325. d) C. Wattanakit, T. Yutthalekha, S. Assavapanumat, V. Lapeyre, A. Kuhn. *Nat. Commun.* 2017, 8, 2087.
- [15] a) L. Yang, C. Chen, X. Liu, J. Shi, G. Wang, L. Zhu, L. Guo, J. D. Glennon, N. M. Scully, B. E. Doherty. *Electrophoresis*. 2010, 31, 1697-1705. b) M. C. Breadmore, R. M. Tubaon, A. I. Shallan, S. C. Phung, A. S. Abdul Keyon, D. Gstoettenmayr, P. Prapatpong, A. A. Alhusban, L. Ranjbar, H. H. See, M. Dawod, J. P. Quirino. *Electrophoresis*. 2015, 36, 36-61.
- [16] D. B. Gordon, G. A. Lord. *Rapid. Commun. Mass. Spectrom.* 1994, 8, 544-548.
- [17] G. A. Lord, D. B. Gordon, L. W. Teiler, C. M. Carr, *J. Chromatogr. A*. 1995, 700, 27-33.